Proc. NIPR Symp. Antarct. Meteorites, 1, 231-246, 1988

MAGNETIC AND METALLOGRAPHICAL STUDIES OF THE BOCAIUVA IRON METEORITE

Minoru FUNAKI[1], Isamu TAGUCHI[2], J. DANON[3], Takesi NAGATA[1]* and Yuji KONDO[4]

[1]*National Institute of Polar Research, 9-10, Kaga 1-chome, Itabashi-ku, Tokyo 173*
[2]*National Museum of Japanese History, Jyonai 117, Sakura 285*
[3]*National Observatory, 77 Rua General Jose, Cristino, Sao Cristovao, Rio de Janeiro, Brazil*
[4]*Japan Electron Optics Laboratory Co., Ltd., 1418 Nakagami-cho, Akishima-shi, Tokyo 196*

Abstract: The Bocaiuva iron meteorite (IAB) has been studied magnetically and metallographically in order to understand its stable natural remanent magnetization (NRM). This meteorite consists of a large amount of 6–7 wt% Ni kamacite, associated with taenite, plessite, schreibersite and magnetite. Tetrataenite less than 0.2% in volume occurs along the high-Ni taenite lamellae and in the kamacite domain walls beside its lamellae. The NRM direction is almost parallel to a dominant plane of tetrataenite development. The Bocaiuva may have acquired the NRM in the slow cooling process under 300°C of the meteorite's parent body or after shock heating by collisions.

1. Introduction

The Bocaiuva iron meteorite has been defined as an IAB meteorite. It is unique in its structure which contains about 10 to 15% by volume of silicate inclusions, surrounded by kamacite (6.5 wt% Ni), (DESNOYERS *et al.*, 1985). Taenite, plessite, chromite, schreibersite and pyrrhotite have been reported. A Widmanstätten pattern of 0.1–0.3 mm wide kamacite bands and Neumann bands are present. Magnetite, probably maghemite, and geothite are often found at the metal-silicate boundaries and are observed to fill the craks of metal and silicates. Although CURVELLO *et al.* (1983) reported troilite in this meteorite, pyrrhotite has been found instead of troilite (DESNOYERS *et al.*, 1985). Forsterite, enstatite and diopside are observed in the silicate inclusions, as well as an unusual interstitial Ca-rich plagioclase. The Mössbauer spectra of a thin slice sample and an extracted sample by HCl from the Bocaiuva show only the kamacite and disordered taenite with 33 to 36% Ni contents, respectively (ARAUJO *et al.*, 1983). Scorzelli and Danon (1986) reported taenite and schreibersite in the extracted materials by HCl. There is no evidence of the presence of ordered FeNi tetrataenite phase by Mössbauer spectroscopy, which suggests a rather fast cooling rate of the meteorite. The authors have investigated the Bocaiuva magnetically and metallographically in order to understand the stability of its natural remanent magnetization (NRM).

In order to interpret the results obtained we performed a detailed investigation by

* Professor Emeritus. Present address: 66, Akagishitamachi, Shinjuku-ku, Tokyo 162.

conventional metallographical method and electron microprobe analysis of the metal phase composition in the Bocaiuva. The Bitter pattern method for investigating the magnetic phases of the meteorite has been used with magnetic fluid applied to the polished surface of the meteorite.

2. Magnetic Properties

2.1. Natural remanent magnetization (NRM), AF and thermal demagnetizations

The original NRM of a bulk sample of the Bocaiuva has been found to be 1.519 $\times 10^{-2}$Am^2/kg by using a spinner magnetometer. The bulk sample A (0.071 g) was demagnetized up to 50 mT by a 3-axis AF demagnetizer. The original NRM intensity decreased steeply by 5 mT, then gradually to 50 mT. The variations of NRM components using a Zijderveld projection are shown in Fig. 1a. The components decompose in three stages; the first stage is a relatively soft magnetic component up to 10 mT characterized by large demagnetization of vertical component; the second stage is a stable one from 10 to 40 mT shifting toward zero for the horizontal components and shifting horizontally for the vertical component; the third stage is a relatively stable one from 40 to 50 mT shifting flat for the both components. The change of NRM directions, as shown in Fig. 1b, represents the stable NRM between 10 and 40 mT, whereas the median demagnetization field (MDF) value of this sample is about 5 mT. Bulk sample B (2.800 g) was AF demagnetized to 14 mT, suggesting stable NRM from 10 to 30 mT with the MDF value of less than 5 mT. However, the NRM directions changed along

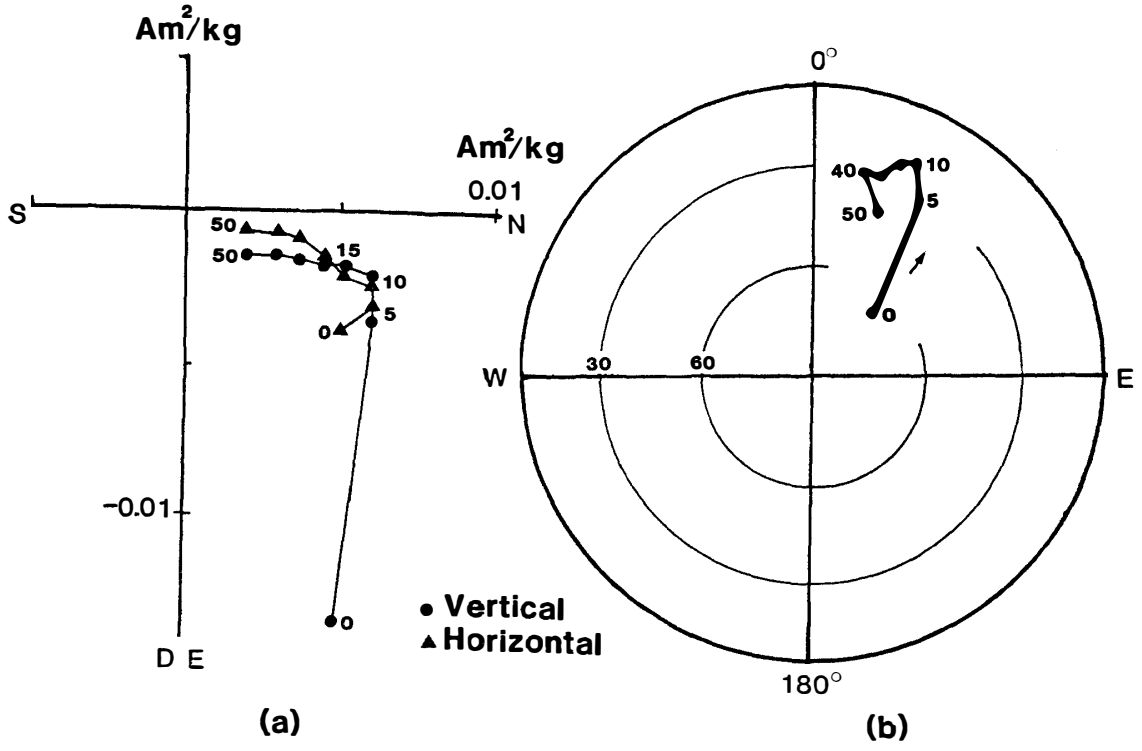

Fig. 1. AF demagnetization curves of a bulk sample of Bocaiuva. (a) Zijderveld projection of NRM components. (b) The directional changes of NRM.

a perpendicular plane of a great circle.

Samples C, D, and E were thermally demagnetized from 50 to 750°C in steps of 50°C in the atmosphere. The changes of NRM intensities and directions are shown in Fig. 2. Sample C (0.482 g), having only stable NRM component in the AF demagnetization to 15 mT, has relatively stable NRM between room temperature and 550–600°C; the intensity (4.760×10^{-3}Am^2/kg) decreases smoothly to 550°C and the directions change within a small area up to 600°C. However, unstable NRM is observed from 550–600 to 750°C. A NRM-blocking temperature is defined at 550°C. Sample D (0.368 g) is the original sample having 3.045×10^{-2}Am^2/kg which is about 10 times stronger than those of samples C and E. The NRM intensity varies little from room temperature to 300°C but then decreases abruptly from 300 to 500°C. The directional change is small from room temperature to 500°C and is large from 550 to 750°C. The NRM-blocking temperature is defined clearly at 550°C. Sample E (0.694 g) is also the original one with 2.940×10^{-3}Am^2/kg. This sample has similar thermal demagnetization character-

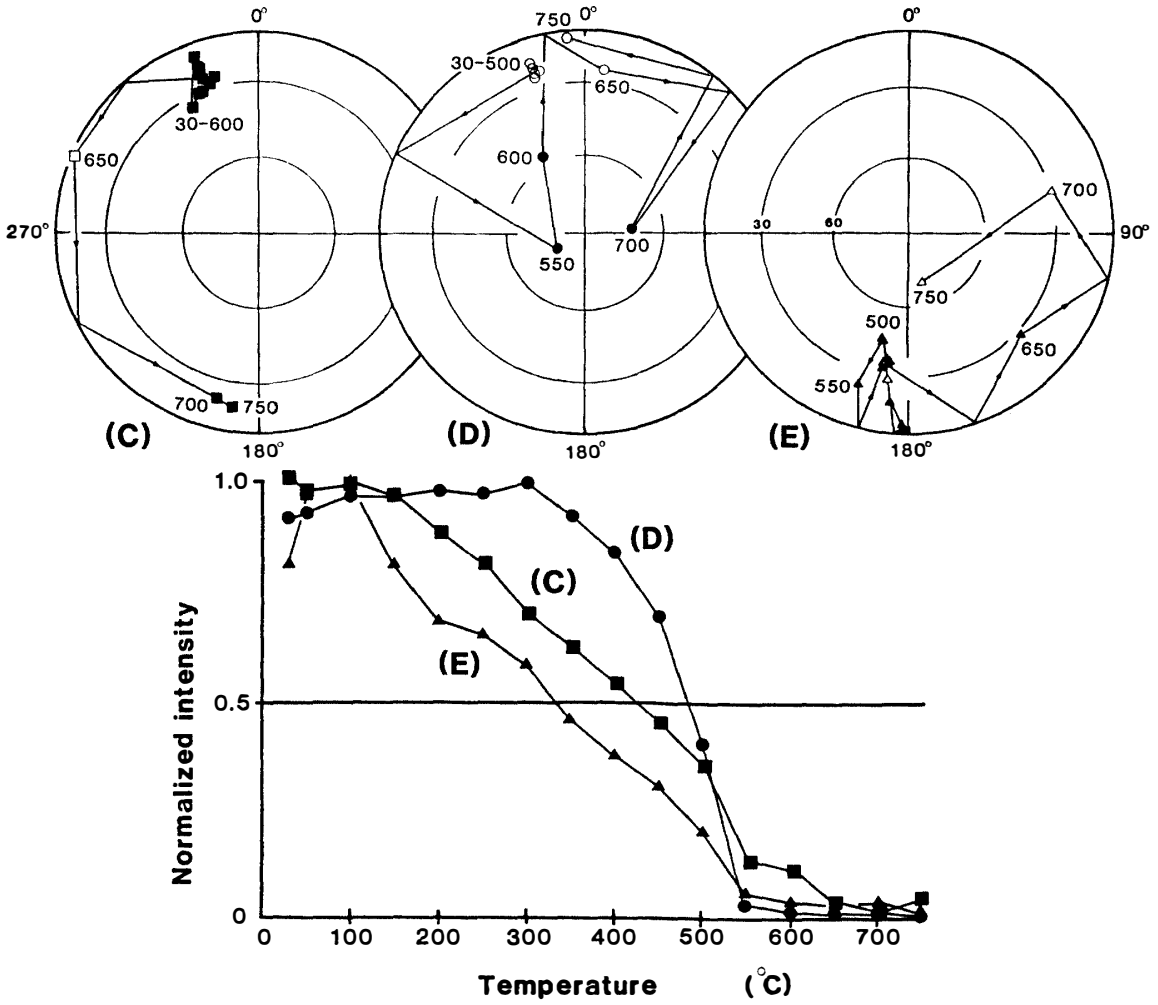

Fig. 2. Thermal demagnetization curves of directions and intensities for three bulk samples. Sample (C): Already demagnetized to 15 mT before the thermal demagnetization. Samples (D) and (E): Original NRM.

istics to those of sample C, except some soft magnetic components observed between room temperature and 150°C.

2.2. Distribution of NRM directions

A total of 22 samples with orientations, ranging from 0.071 to 2.8 g in weight, are prepared from a block sample of the Bocaiuva. The original NRM of every sample was measured, and subsequently 18 samples were AF demagnetized by 15 mT, which is the optimum AF demagnetization field intensity, for removing the relatively soft NRM components (the first stage of AF demagnetization).

The variations of the NRM intensities are fairly large among the samples, such as 1.1×10^{-1} to 4.6×10^{-3}Am^2/kg for the original samples and 1.4×10^{-2} to 4.4×10^{-3}Am^2/kg after the AF demagnetization. The respective average intensities are order of 10^{-2} and 10^{-3}Am^2/kg. The weaker or stronger NRM intensities are distributed randomly in the block sample. The NRM directions before and after that demagnetization are distributed as shown in Fig. 3. The distribution before the demagnetization shows a tendency of alignment approximately along a great circle over a hemisphere. This tendency does not change by the demagnetization, although the NRM directions of a few samples shift widely within the great circle by the demagnetization. It suggests that both of the hard and the relatively soft magnetic components of the Bocaiuva have been magnetized to the directions within the same plane.

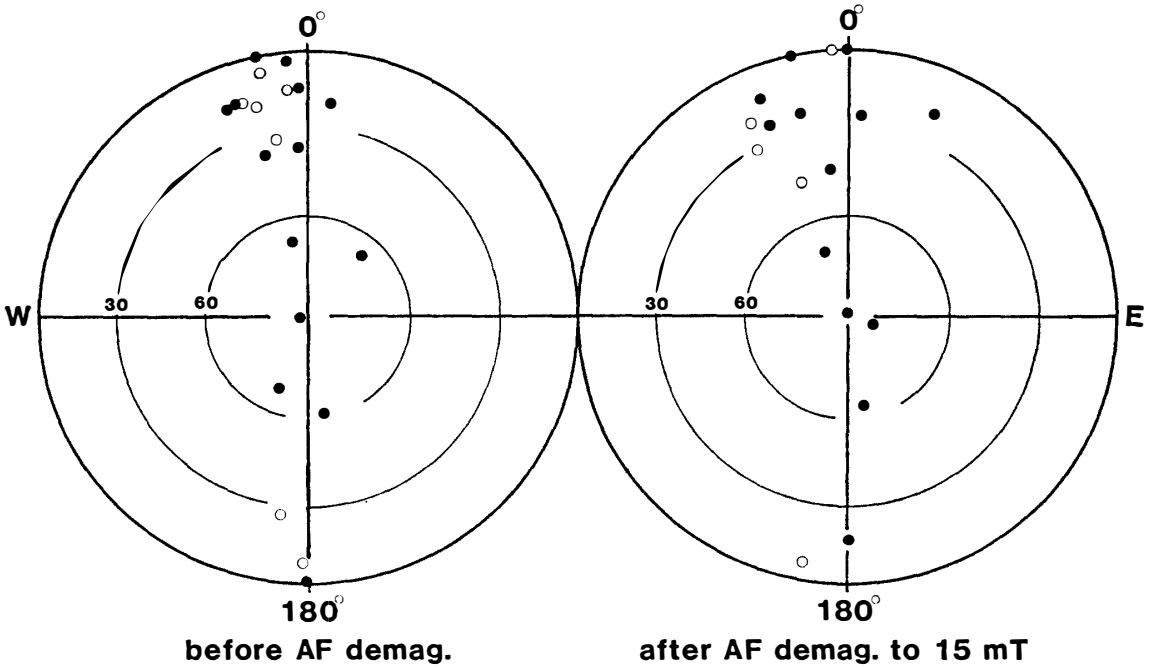

Fig. 3. Distributions of NRM directions for bulk samples before and after AF demagnetization to 15 mT. Open circle: upward direction, solid circle: downward direction.

2.3. Magnetic hysteresis properties and the thermomagnetic curves

Magnetic hysteresis properties and thermomagnetic curves have been measured with bulk 1 and 2 samples and an extracted sample by HCl from the Bocaiuva meteorite.

Table 1. Magnetic hysteresis properties and Curie points of Bocaiuva.

Sample	Heating	I_S Am^2/kg	I_R Am^2/kg	H_C mT	H_{RC} mT	Tc heating °C	Tc cooling °C
Bulk 1	before	205.5	0.5	4	<5	760	610~450
	after	209	0.02	1.5	<5	725	605
Bulk 2	before	201	0.035	2.5	<5	745	605
	after	212	0.04	1.0	<5	735	605
Lamella	before	87.5	1.5	23.5	66.7	310, 550	255
	after	82.5	0.005	1.0	<5	290	260

Magnetic hysteresis properties, saturation magnetization (I_S), saturation remanent magnetization (I_R), coercive force (H_C) and remanence coercive force (H_{RC}) were determined using the magnetization curve from -1.4 to $+1.4$ T in a steady magnetic field at room temperature. These values before and after heating up to 850°C are listed in Table 1, whereas the values of H_{RC} could not be obtained due to the weaker magnetization than the noise level (about 5 mT). The principal magnetic mineral in both bulk samples appears to be low Ni of FeNi alloys judging from their large I_S values (205.5 and 201 Am^2/kg for samples 1 and 2, respectively). Small values of I_R and H_C may suggest a multidomain structure of their principal magnetic minerals. These magnetic characteristics do not change obviously by the heating treatment to 850°C. For the extracted samples, however, large values of H_C and H_{RC} (23.5 and 66.7 mT respectively) have been observed, and the values decreased markedly ($H_C = 1.0$ and $H_{RC} <$ 5 mT) after heating to 650°C. These marked changes of H_C and H_{RC} values by heat treatment are explained only by the existence of a tetrataenite phase in the extracted sample.

Thermomagnetic curves (I_S-T curves) from room temperature up to 850°C are obtained under 10^{-2} Pa atmospheric pressure, 200°C/h of heating and cooling rates and 600 mT of steady magnetic field. Obtained 1st and 2nd run curves are shown in Fig. 4 and the Curie points are listed in Table 1. The 1st run I_S-T curve of bulk 1 sample shows phase transition temperature from bcc to fcc ($\alpha \rightarrow \gamma$) at 760°C and from fcc to bcc ($\gamma \rightarrow \alpha$) at 610°C suggesting 6%Ni FeNi alloy for the main magnetic mineral. A slight gradual change of the Curie point around 450°C was observed in the cooling curve. In the 2nd run I_S-T curves, the phase transition temperature decreases at 725°C ($\alpha \rightarrow \gamma$) and at 605°C ($\gamma \rightarrow \alpha$) suggesting an increase of the Ni content to 8% in kamacite by the heat treatment. The Curie point observed at about 450°C in the 1st run cooling curve disappears in the 2nd run curve, so that it is an unstable phase produced by the heat treatment to 850°C. In the case of bulk sample 2, observed phase transition temperatures are 745°C ($\alpha \rightarrow \gamma$) and 605°C ($\gamma \rightarrow \alpha$) for the 1st run cycle and 735°C ($\alpha \rightarrow \gamma$) and 605°C ($\gamma \rightarrow \alpha$) for the 2nd run cycle. It suggests that bulk sample 2 consists of 7 wt% Ni kamacite originally and 8 wt% Ni kamacite after heating to 850°C.

The I_S-T curves of the extracted samples are irreversible with the Curie points at about 310 and 550°C in the heating curve and at about 255°C in the cooling curve. The main Curie points at about 310 and 255°C can be attributed to the taenite with 34–36% Ni. It is also possible the Curie points result from schreibersite, since this mineral has a Curie point of about 300°C. The I_S-T curve is very flat from 350 to

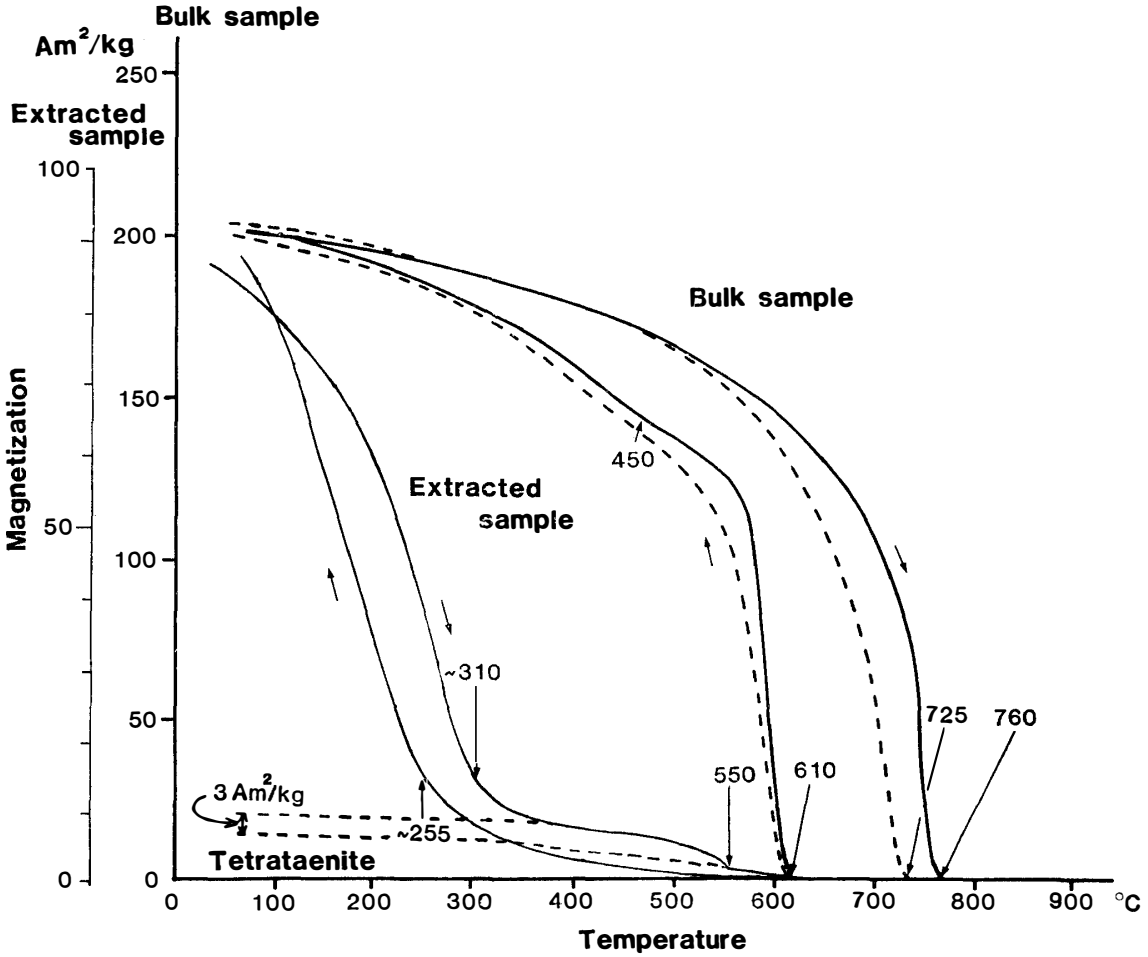

Fig. 4. Thermomagnetic (I_S-T) curves of a bulk sample and an extracted sample by HCl obtained by 0.6T external magnetic field. Solid curves: 1st run I_S-T curves dotted curves: 2nd run I_S-T curves.

500°C, then it decreases abruptly up to 550°C, while there is no significant Curie point around 550°C in the cooling curve. Characteristics of the I_S-T curves between 350 to 550°C are typical I_S-T cruves of the tetrataenite phase.

The extracted sample of 0.01305 g (2.7%) was obtained from 0.482 g of the bulk Bocaiuva sample. It may be concluded that the sample included the tetrataenite phase judging from the I_S-T curves and the magnetic hysteresis properties. If the I_S-T curves resulting from the tetrataenite phase can be estimated as shown in Fig. 4, the magnetization intensity of that phase is about 3 Am²/kg. Since the saturation magnetization of 50%Fe 50%Ni alloy is 85.5 Am²/kg, the calculated amount of tetrataenite phase is found to be about 0.1% in weight, when the tetrataenite can be supposed to be almost saturated at 0.6 T of external magnetic field. Usually tetrataenite is not saturated by the field of 0.6 T, but the magnetization shows more than half of the saturation magnetization. It may be, therefore, that the Bocaiuva includes tetrataenite phase less than 0.2 wt% in the bulk sample.

3. Metallography

3.1. Microscopical observations

A sample of the Bocaiuva, about 10×5 mm^2 in area, has been polished and slight etched with Nital. Octahedrite structures on the surface were observed by a metallographical microscope under bright (Fig. 5a) and dark fields (Fig. 5b). Clusters of many isolated or jointed silicate inclusions of less than 1 mm in diameter are swathed by kamacite, schreibersite or iron-sulphide. It seems likely that the development of Widmanstätten patterns 0.1–0.3 mm wide is disturbed by the silicate inclusions. The Neumann bands are developed in the kamacite phase, especially in that surrounded by the inclusions. Schreibersite and iron-sulphide are observed only at the contact with the inclusions. Iron oxide is often found at the grain boundaries and filled in the cracks of silicate, schreibersite, iron-sulphide and rarely kamacite. Lamellar taenite,

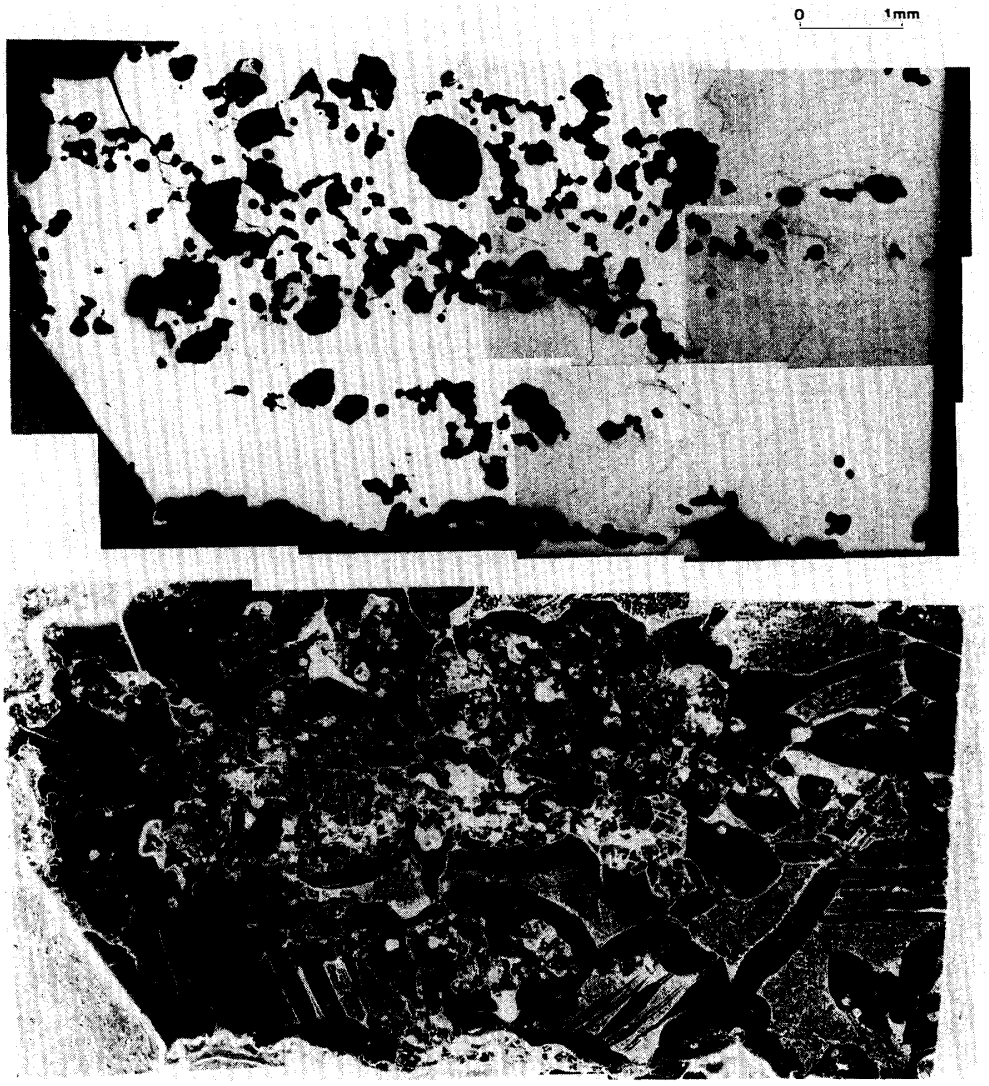

Fig. 5. Silicate inclusions and Widmanstätten patterns of Bocaiuva taken by bright field (up) and dark field (down) microscope.

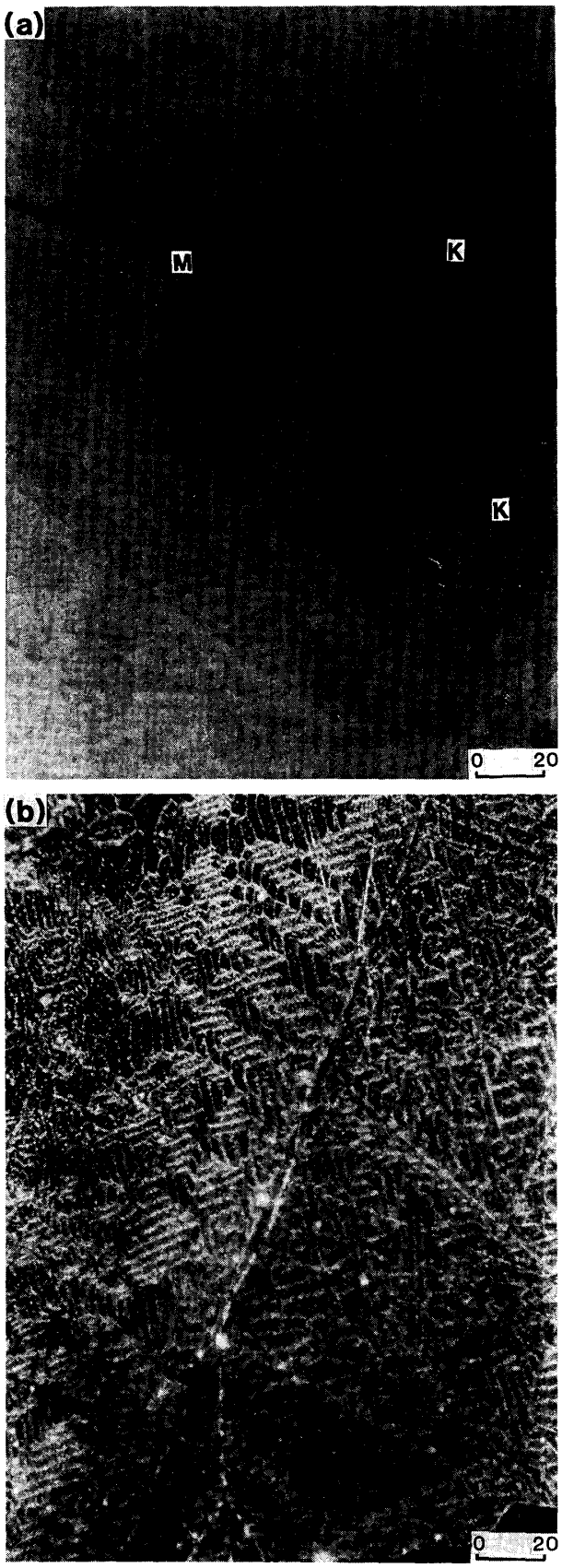

Fig. 6. Features of strong NRM regions of Bocaiuva by Bitter pattern method.
Scale: μm, K: kamacite, T: taenite, TT: tetrataenite, M: magnetite.

(a, b) Configurations of magnetic domains of kamacite ((a) bright, (b) dark fields).

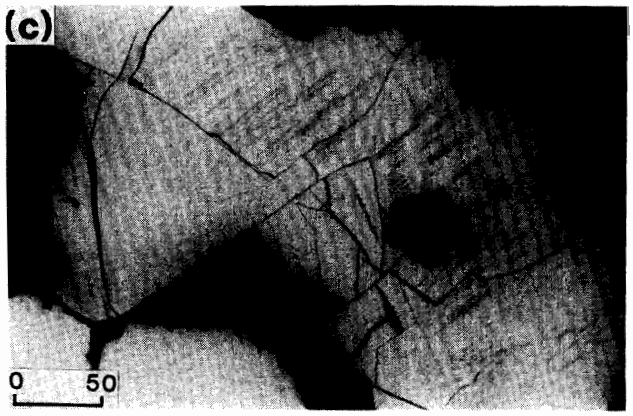

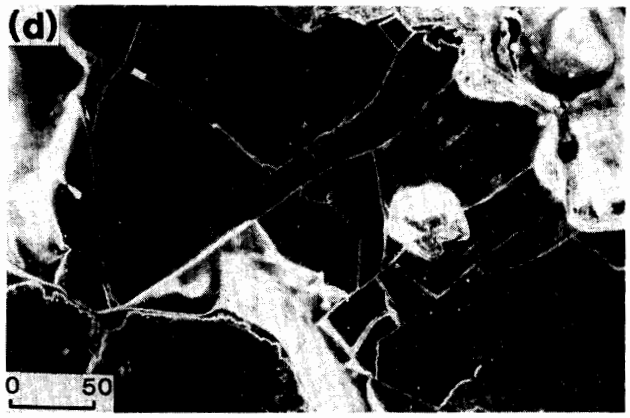

(*c, d*) *Configurations of magnetic domains taken under bright field* (*c*) *and dark field* (*d*) *of schreibersite.*

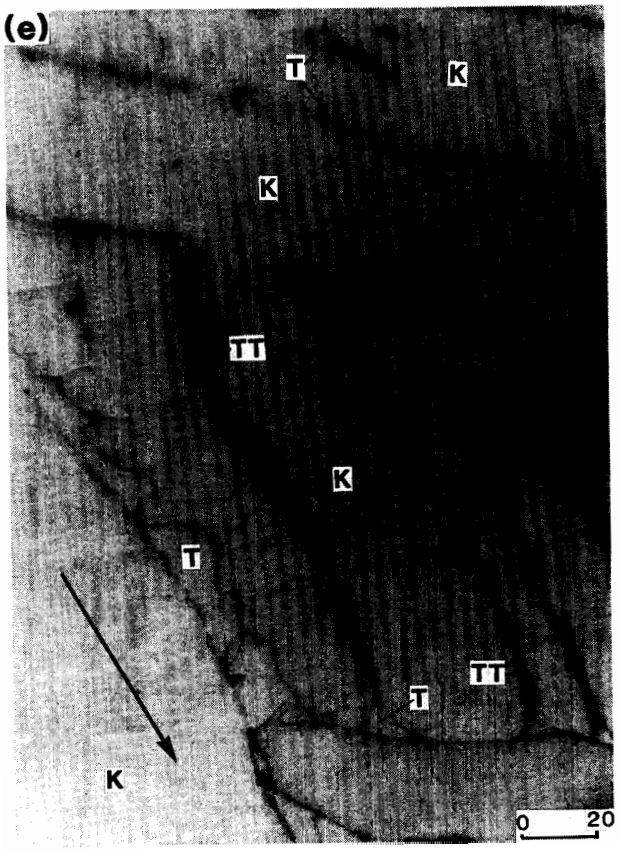

(*e*) *Extremely strong NRM lamellae* (*tetrataenite*) *and the NRM direction* (*arrow*) *of the sample.*

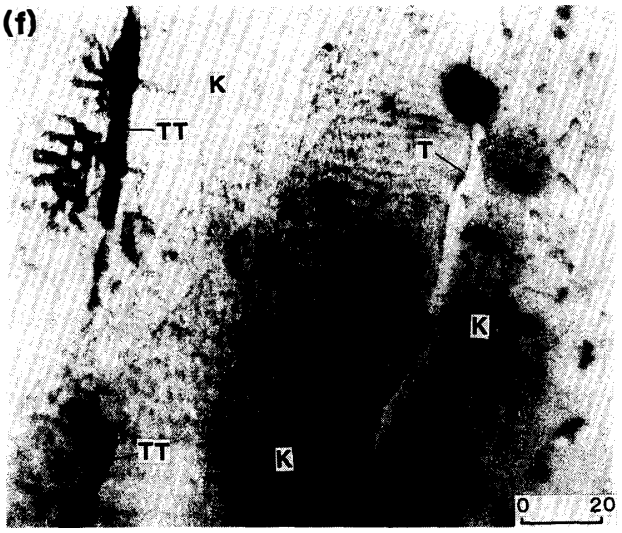

Fig. 6. (f) Branched out of extremely strong NRM twigs (tetrataenite) into the kamacite field through domain walls from tetrataenite lamella.

5–40 μm thick, appears along the limbs of plessite and kamacite lamellae. Spheroidal the taenites, 5–10 μm in diameter, are distributed commonly in the wide area of the plessite field. Acicular taenites clearly and less clearly defined, 20–10 μm in length, appear also in the plessite field. These taenites do not show optical anisotropy under reflected light. The plessite, more than 1 mm in size, is observed commonly in the Bocaiuva. It disappears in the clusters of silicate inclusion.

3.2. Identification of NRM carriers by Bitter pattern method

In order to study the magnetic carriers in the Bocaiuva we used the Bitter pattern method. The polished surface of the meteorite was painted with a magnetic fluid which is a coloidal suspension of magnetite (about 200 Å particle diameter). Figure 6 shows the Bitter pattern configuration of magnetic domains on the surface of kamacite, schreibersite and taenite lamellae. The domain structure of kamacite (5–10 μm wide and 5–20 μm long in each lath) shows parallel alignments or eddy patterns being composed of straight laths. After thermal demagnetization to 750°C, these systematic ordered configurations of the domain structure collapse. The domain on schreibersite (under 10 μm wide and 100 μm long) shows a parallel alignment having internal zigzag deformations. No correlation is observed between these domain configurations of kamacite and schreibersite and the NRM directions of the Bocaiuva. Small concentration of the magnetic fluid appears on the magnetite veins, although no magnetic fluid concentration appears on the iron-sulphide grains.

The magnetic fluid concentrates densely along the borders of some taenite lamellae suggesting a strong NRM carrier. The concentration consists of linking elliptical speckles which have no such internal structures as magnetic domains. From the speckles fine twigs of the concentration branched out into the kamacite field along the kamacite domain walls. The dominant direction of these lamellae is almost parallel to the NRM direction, These taenites taking strong NRM disappear after heat treatment at 650°C. The phenomenon is similar to the thermal disordering of tetrataenite lamellae in the Toluca iron meteorite reported by FUNAKI *et al.* (1986).

4. EPMA and CMA Analyses

DESNOYERS *et al.* (1985) reported chemical compositions of silicates, pyrrhotite and schreibersite in the Bocaiuva, with some measurements for the FeNi phases. We measured the chemical compositions in detail of the metallic phases as summarized in Table 2. Kamacite of the selected 4 points (point 1–4) from the different grains consists of 92–93 wt% Fe, 6–7 wt% Ni, 0.5 wt% Co, and small amounts of P, Cu and Zn suggesting almost homogeneous composition among grains. Measurement points for taenite (points 5, 6 and 7) were selected from lamellar taenite which did not show the heavy concentration of magnetic fluid (weak NRM lamellae). The taenite lamellae have 78.0–81.5 wt% Fe, 17.5–21.2 wt% Ni, 0.1–0.3 wt% Co and small amounts of P, S and others; the Ni content is very different among the lamellae. Point 8 is a taenite lamella showing haevy concentration of magnetic fluid (strong NRM lamella). At this point we observed the highest Ni content (37.6 wt% Ni) in FeNi metals. Other elements in this lamella do not much differ compared with the weak NRM lamellae. Points 9 and 10 selected from spheroidaized taenite in the plessite field are about 86.5 wt% Fe, 12 wt% Ni and 0.4 wt% Co for main compositions. The compositions of a total of 7 points from schreibersite show variation of 78.0–81.5 wt% Fe and 17.4–21.2 wt% Ni and relatively homogenized 15.3–15.8 wt% P.

Table 2. Chemical compositions of iron-nickel and schreibersite grains analyzed by EPMA, 1–12: this study; a-h: DESNOYERS et al. (1985). (unit wt%)

No.	Fe	Ni	Co	P	S	Cu	Zn	Total
Kamacite								
1	92.428	6.839	0.533	0.100	0.005			99.905
2	92.417	6.950	0.499	0.043	0.021			99.930
3	92.094	6.896	0.510	0.093	0.000			99.593
4	93.541	6.150	0.562	0.136	0.007			100.396
a	91.9	6.65	0.35	0.18		0.06	0.03	99.17
b	92.7	6.51	0.34	0.05		0.05	0.03	99.68
Taenite lamellae								
5	81.454	17.482	0.334	0.042	0.001			99.314
6	81.163	17.935	0.332	0.009	0.018			99.456
7	78.023	21.158	0.349	0.016	0.030			99.576
c	81.2	17.6	0.14	0.02		0.28	0.03	99.27
8	61.043	37.613	0.142	0.021	0.010			98.828
Plessite								
9	86.566	11.874	0.419	0.048	0.013			98.920
10	86.526	12.175	0.404	0.024	0.005			99.133
Schreibersite								
11	59.816	24.968	0.192	15.808	0.070			100.854
12	55.232	28.437	0.190	15.584	0.084			99.528
d	61.0	22.2	0.07	15.3	0.08	0.14	0.74	99.53
e	56.6	26.9	0.05	15.5	0.06	0.12	0.74	99.97
f	54.3	29.0	0.04	15.5	0.07	0.15	0.72	99.78
g	52.0	31.5	0.04	15.5	0.06	0.13	0.73	99.96
h	43.8	39.5	0.03	15.4	0.06	0.15	0.72	99.66

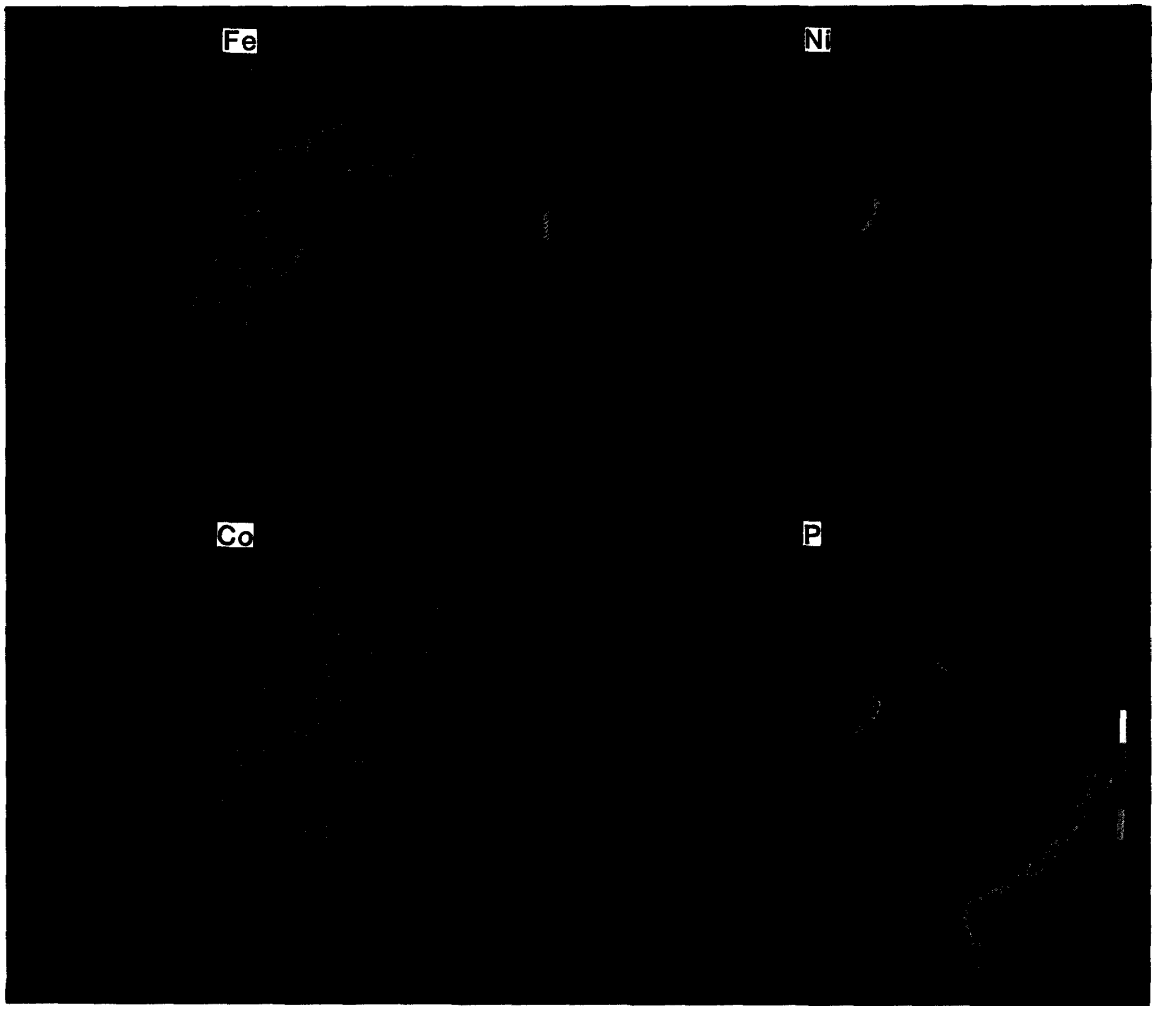

Fig. 7. Elemental distribution patterns of Fe, Ni, P and on Bocaiuva by computer-aided micro-analyzer (CMA).

Elemental distribution patterns of Fe, Ni, Co and P from two fields (1.0×0.67 mm) were mapped using a computer-aided microanalyzer (CMA). The number of dots in the patterns are 250 for length and 200 for side, and the beam diameter is 5 μm. One of the fields including kamacite, lamellar taenite, plessite, schreibersite and silicate inclusions is shown in Fig. 7. Concentrations of the above elements and their area in the two fields are listed in Table 3. In this picture, kamacite consists of 85–95 wt% Fe, 5–8 wt% Ni, 0.3–0.8 wt% Co and less than 0.5 wt% P. In general, uniform chemical composition of the kamacite phase is observed, although relatively low Ni dots (85–90 wt% Fe) are distributed in the wide area of 90–95 wt% Fe content. The lamellar taenite consists of 50–85 wt% Fe, 15–35 wt% Ni, 0.2–0.4 wt% Co and less than 0.5 wt% P. There is a negative correlation between Fe and Ni; high Fe area includes low Ni. The plesssite consists of 70–90 wt% Fe, 5–30 wt% Ni, 0.2–0.8 wt% Co and less than 0.5 wt% Co. In the plessite clearly distinguished zoning patterns of Fe, Ni and Co are observed from the center to the limb; Ni contents increase toward the limb, whereas Fe and Co contents decrease. The Ni content in the limb of plessite extremely decreases around schreibersite. It seems likely that the Ni in plessite was absorbed by schreibersite. Schrei-

Table 3. Element concentrations and their occupied areas.

	Color	Fe		Ni		Co		P	
		conc. wt%	area %	conc. wt%	area %	conc. wt%	area %	conc. wt%	area %
Field 1	White	95.0	0.00	35.0	0.11	1.0	0.01	18.0	0.00
	Pink	95.0	48.57	35.0	0.63	1.0	0.89	18.0	0.01
	Red	90.0	27.33	30.0	3.35	0.8	24.11	16.0	0.50
	Yellow	85.0	5.45	22.0	4.64	0.6	32.25	14.0	0.63
	Green	80.0	3.02	15.0	11.21	0.5	19.44	12.0	0.63
	Sky-blue	75.0	1.84	8.0	67.66	0.4	7.73	8.0	0.60
	Blue	70.0	2.74	5.0	1.97	0.3	3.08	3.0	0.59
	Black	50.0	11.06	2.0	10.25	0.2	12.49	0.5	97.06
	Total	79.0710		7.5419		0.4548		0.3137	
Field 2	White	95.0	0.01	35.0	0.00	1.0	0.00	18.0	0.02
	Pink	95.0	34.18	35.0	0.29	1.0	1.31	18.0	1.22
	Red	90.0	7.46	30.0	7.17	0.8	19.21	16.0	10.64
	Yellow	85.0	0.60	22.0	11.15	0.6	14.39	14.0	3.86
	Green	80.0	0.53	15.0	1.83	0.5	7.54	12.0	2.75
	Sky-blue	75.0	0.46	8.0	35.29	0.4	2.85	8.0	1.94
	Blue	70.0	19.28	5.0	8.73	0.3	6.95	3.0	2.61
	Black	50.0	37.48	2.0	35.54	0.2	47.75	0.5	76.97
	Total	53.1934		6.6292		0.2404		2.7573	

bersite consists of less than 70 wt% Fe, more than 15 wt% Ni, less than 0.3 wt% Co and 3–16 wt% P. The average percentages of the elemental concentrations in this picture (including silicate area) are 79.0710% Fe, 7.5419% Ni, 0.4548% Co and 0.3137% P.

5. Discussion

Bulk samples of the Bocaiuva have very small coercivity (H_C=1.5–4.0 and $H_{RC}<$ 5 mT). The main magnetic mineral would be 6–7 wt% Ni in kamacite analyzed by I_S-T curves. The value is supported by the EMPA and CMA analyses. As the secondary magnetic minerals, taenite, plessite, magnetite and schreibersite exist in the Bocaiuva as determined by the EPMA and CMA analyses and by the microscopic observations using the Bitter pattern method. However, pyrrhotite may be nonmagnetic at room temperature due to the absence of characteristics of ferrimagnetic pyrrhotite in the I_S-T curves and evidence of any concentration of magnetic fluid on its surface.

However, extracted samples have extremely high coercivities (H_C=23.5 and H_{RC}= 66.7 mT) which decrease (H_C=1 and $H_{RC}<$5 mT) by heat treatment at 650°C. This characteristic of the coercivity change is consistent with that of typical tetrataenite (NAGATA *et al.*, 1986). The I_S-T curves of the samples show the main Curie point at 310°C of schreibersite or taenite which includes nickel about 34–36 wt%. Probably this point overlaps the Curie points of taenite and schreibersite. Because, for obtaining the extracted samples we used the same technique as the one employed by SCORZELLI and DANON (1986) who obtained the overlap pattern of taenite (33–36 wt% Ni; ARAUJO *et al.*, 1983) and the spectrum of schreibersite (22.2–39.5 wt% Ni) by the Mössbauer

analyses of the extracted samples from the Bocaiuva. The I_S-T curves of the extracted samples show a minor amount of tetrataenite phase, which are characteristically flat from 300 to 550°C with a Curie point at 550°C only in heating curves. The microscopical observations with magnetic fluid and EPMA analyses showed high-nickel taenite lamellae (37.6 wt% Ni) which had very strong NRM. FUNAKI *et al.* (1986) reported the extremely strong NRM resulting from tetrataenite using extracted lamellae of the Toluca. The magnetic characteristics of the lamellae of Toluca are essentially consistent with those of the Bocaiuva. The Mössbauer spectrum of the Toluca lamellae (ALBERTSEN *et al.*, 1978) indicated a superposition of a paramagnetic-phase spectrum and an asymmetric six-line spectrum from the ordered phase. Since the tetrataenite is atomically ordered FeNi which is tetragonal superlattice, the Ni content must be 50 wt%. Probably the 37.6 wt% Ni content of tetrataenite in the Bocaiuva is due to mixture of fine-grained tetrataenite, and paramagnetic taenite in the case of the Toluca.

From these viewpoints, the Bocaiuva includes a small amount of tetrataenite less than 0.2 wt%, as discussed in Section 2.3, without doubt. No ditection of tetrataenite in bulk samples seems due to its extremely small amount as compared with kamacite. Even with the extracted sample by HCl, tetrataenite might not be detected in the previous Mössbauer analyses (ARAUJO *et al.*, 1983; SCORZELLI and DANON, 1986), because the overlap with the much more intense lines of the Ni-rich disordered taenite phase.

Essentially the NRM in the Bocaiuva is very stable against AF demagnetization suggesting its relation with the high coercivity of magnetic minerals. As the NRM decays completely by thermal demagnetization at 550°C, the NRM may result from mainly tetrataenite. Although there are some possibility of disordered taenite having 50 wt% Ni with Curie point at 550°C, its contribution to NRM may be small because 50 wt% Ni is not detected by the EPMA and CMA analyses. BRECHER and ALBRIGHT (1977) pointed out that all magnetization directions in octahedrites appear to be preferentially associated with the octahedral (111) crystallographic planes. The NRM directions of 22 block samples of the Bocaiuva are almost parallel to a dominant plane of lamellar tetrataenite development of the (111) plane. DUBOIS (1965) studied the magnetic domain configurations of kamacite and schreibersite in Odessa (coarsest octahedrite) and reached the conclusion that the NRM and the configuration are roughly related with each other. However, any obvious correlation between the domain configurations and the NRM directions could not be observed for the Bocaiuva. These experimental results of NRM strongly support that tetrataenite is the NRM carrier for the Bocaiuva.

According to BRECHER and ALBRIGHT (1977), the stabilities of NRM against AF demagnetization of octahedrite meteorites increase systematically from the coarser to the finer-grained classes. The kamacite plates of the Bocaiuva range in width from 0.1 to 1.3 mm suggesting the finest octahedrite, so that the NRM of the Bocaiuva is estimated to be unstable. The intensity of relatively stable NRM component against AF demagnetization up to 10 mT (first stage) observed was about half of the original NRM intensity. The directions are roughly parallel to the development plane of lamellar tetrataenite, because the NRM direction patterns of block samples before and after AF demagnetization to 15 mT (Fig. 3) are essentially consistent with each other. The amount of kamacite is much larger than that of other magnetic minerals in the

Bocaiuva as shown in Fig. 7. On the surface of the kamacite the magnetic multidomain structures appear clearly by the Bitter pattern method. It may be, therefore, that the kamacite should contribute to the NRM of the Bocaiuva. However, it cannot be seen that the NRM from kamacite of multidomain structures affects the Bocaiuva strongly due to the good NRM stability. The NRM stability of the Bocaiuva must be worth judging from $H_C=2.5$–4 and $H_{RC}<5$mT.

Among the octahedrite meteorites having kamacite, as the main magnetic mineral, relatively stable NRM against AF demagnetization has been found in Y-75031, Y-75105 and ALH-762 (NAGATA, 1979), whereas their coercivities are extremely small. As the former two meteorites are of a very small size, they acquired the stable TRM probably through the earth's atmosphere in the presence of the geomagnetic field. ALH-762 is large enough size and a magnetic sample was obtained sufficiently from its fusion crust, suggesting no possibility of heating by the earth's atmosphere. The measured samples of the Bocaiuva were obtained from the meteorite's interior and the NRM characteristics are very similar to those of ALH-762. On the other hand, the Toluca (medium octahedrite) has extremely unstable NRM, although it includes a relatively large amount of tetrataenite compared with the Bocaiuva. These experimental evidences suggest that the contribution of kamacite to NRM differs among octahedrite meteorites.

In the case of the Bocaiuva, the weak contribution of kamacite to NRM may be ascribed to the following possibility. The NRM directions of kamacite magnetic domains are completely random, so that the integrated NRM can be ignored due to negation of their NRM in comparison with that of tetrataenite. As the strong NRM twigs invaded in the kamacite field through the domain walls, there is a possibility that the high coercivity minerals (tetrataenite) spread over the wide area of the kamacite field in the Bocaiuva, although the concentration cannot be distinguished from kamacite magnetic domains due to scattering these minerals. The concentration of Ni in the kamacite phase is 6–7 wt% estimated by I_S-T analyses, but after heat treatment at 850°C it increased to 8 wt%. It suggests that Ni diffused into the kamacite from the side of high-Ni fine grains. If there are fine grains of high coercivity taenite in the kamacite domain walls, the diffusion is plausible.

DESNOYERS *et al.* (1985) clarified that the Bocaiuva cooled rapidly from 1100°C to the temperature where the diffusion in the silicates stopped, then it must be cooled slowly down to 600°C due to the presence of Widmanstätten patterns. From our magnetic and metallographical results, the existence of a small amount of tetrataenite phase in the Bocaiuva defined that this meteorite further cooled slowly under 300°C. The Bocaiuva has many Neumann bands in the kamacite field representing the shocks caused by collisions. If the temperature increased more than 550°C by the shocks, the previous tetrataenite should be disordered and it reset the tetrataenite forming again. Poor development of the tetrataenite phase may result in this event. Namely, the formation of the tetrataenite phase is disturbed by a faster cooling rate (insufficient time for diffusion) due to mass loss of the parent body by collisions. Another possibility is that the relatively large amount of schreibersite absorbed the Ni from the taenite phase, so that the low Ni content in the taenite phase could not become high enough for creation of tetrataenite.

6. Conclusion

The Bocaiuva has a very stable NRM against AF demagnetization, contradictory to the low H_C and H_{RC} values. The NRM directions are aligned to a plane related to the octahedrite structure. The NRM is broken down by thermal demagnetization at 550°C. Extremely strong NRM lamellae are observed by the Bitter pattern method but they disappear after heat treatment at 600°C. Extracted lamellae have large H_C and H_{RC} values and have the Curie point at 550°C, whereas the coercivity decreases and the Curie point disappears after heating at 600°C. These magnetic behaviors are consistent with those of typical tetrataenite. Both EPMA and CMA analyses and magnetic results revealed the presence of the tetrataenite phase in high-Ni (38 wt%) lamellae. Probably fine tetrataenite exists in small amounts dispersed in the kamacite domain walls beside the tetrataenite lamellae. Tetrataenite may not be detected in the previous Mössbauer results because of the overlap with the much more intense lines of the Ni-rich disordered taenite phase. From these evidences, the Bocaiuva was cooled down slowly under 300°C producing the tetrataenite phase in high-Ni regions.

Acknowledgments

The authors wish to thank Japan Electron Optics Laboratory Co., Ltd. for the chemical analyses by EPMA and CMA of the Bocaiuva meteorite and to thank Nippon Seiko Co., Led. for supplying the magnetic fluid. One of us (J. DANON) is indebted to the Brazilian Antarctic Program (PROANTAR) for enabling him to participate in this work.

References

ALBERTSEN, J.F., JENSEN, G.B. and KNUDSEN, J.M. (1978): Structure of taenite in two iron meteorites. Nature, **273**, 453–454.

ARAUJO, S.I., DANON, J., SCORZELLI, R.B. and AZEVEDO, I.S. (1983): Mössbauer study of silicates and metal phases of the Bocaiuva meteorite. Meteoritics, **18**, 261.

BRECHER, A. and ALBRIGHT, L. (1977): The thermoremanence hypothesis and the origin of magnetization in iron meteorites. J. Geomgn. Geolectr., **29**, 379–400.

CURVELLO, W.S., MALVIN, K.J. and WASSON, J.T. (1983): Bocaiuva, a unique silicate inclusion bearing iron meteorite. Meteoritics, **18**, 285.

DESNOYERS, C., CHRISTOPHE MICHEL-LEVY, M., AZEVEDO, I.S., SCORZELLI, R.B., DANON, J. and GALVÃO DA SILVA, E. (1985): Mineralogy of the Bocaiuva iron meteorite; A preliminary study. Meteoritics, **20**, 113–124.

DUBOIS, R.L. (1965): Some investigations of the remanent magnetism and domain structures of iron meteorites. J. Geomagn. Geoelectr., **17**, 381–390.

FUNAKI, M., NAGATA, T. and DANON, J. (1986): Magnetic properties of lamellar tetrataenite in Toluca iron meteorite. Mem. Natl Inst. Polar Res., Spec. Issue, **41**, 382–393.

NAGATA, T. (1979): Natural remanent magnetization of Antarctic meteorites. Mem. Natl Inst. Polar Res., Spec. Issue, **12**, 238–249.

NAGATA, T., FUNAKI, M. and DANON, J. A. (1986): Magnetic properties of tetrataenite-rich meteorites II. Mem. Natl Inst. Polar Res., Spec. Issue, **41**, 364–381.

SCORZELLI, R.B. and DANON, J. (1986): Mössbauer study of schreibersite from Bocaiuva iron meteorite. Meteoritics, **21**, 509.

(Received November 24, 1987; Revised manuscript received January 20, 1988)